

# Metal-insulator transition above room temperature in maximum colossal magnetoresistance manganite thin films

X. J. Chen,<sup>1,2</sup> H.-U. Habermeier,<sup>2</sup> H. Zhang,<sup>2</sup> G. Gu,<sup>2</sup> M. Varela,<sup>3</sup> J. Santamaria,<sup>3</sup> and C. C. Almasan<sup>1</sup>

<sup>1</sup>Department of Physics, Kent State University, Kent, Ohio 44242, USA

<sup>2</sup>Max-Planck-Institut für Festkörperforschung, D-70569 Stuttgart, Germany

<sup>3</sup>GFMC, Departamento de Física Aplicada III, U Complutense, 28040 Madrid, Spain

(Received 22 June 2004; published 2 September 2005)

It has been suggested that the maximum magnitude of colossal magnetoresistance occurs in mixed-valent manganites with a tolerance factor  $t=0.96$  [Zhou, Archibald, and Goodenough, *Nature (London)* **381**, 770 (1996)]. However, at  $t\approx 0.96$  most manganites have relatively low values of the metal-insulator transition temperature  $T_{MI}$  ( $\sim 60$ – $150$  K). Here, we report that a  $50 \text{ \AA}$   $\text{La}_{0.9}\text{Sr}_{0.1}\text{MnO}_3$  thin film with  $t=0.96$  grown on a (100)  $\text{SrTiO}_3$  substrate has a metal-insulator transition above room temperature, which represents a doubling of  $T_{MI}$  compared with its value in the bulk material. We show that this spectacular increase of  $T_{MI}$  is a result of the epitaxially compressive strain-induced reduction of the Jahn-Teller distortion.

DOI: [10.1103/PhysRevB.72.104403](https://doi.org/10.1103/PhysRevB.72.104403)

PACS number(s): 71.30.+h, 68.55.Jk, 75.47.Gk

## I. INTRODUCTION

The continually increasing demand for low-cost magnetic information storage and retrieval has motivated efforts to improve the performance of relevant hardware compounds. At present, perovskite manganites  $A_{1-x}A'_x\text{MnO}_3$  ( $A$  is a trivalent rare-earth ion and  $A'$  is a divalent alkali-earth ion) are being reexamined as possible next generation magnetic sensor materials due to their colossal magnetoresistance (CMR) effect. Extensive studies<sup>1,2</sup> have shown that the tolerance factor  $t$  [ $t=(r_A+r_O)/\sqrt{2}(r_{Mn}+r_O)$  with  $r_A$ ,  $r_O$ , and  $r_{Mn}$  the radius of the  $A$ -site, oxide, and manganese ions, respectively] is the only parameter which controls the value of both the metal-insulator transition temperature ( $T_{MI}$ ) and CMR. In general,  $t$  has opposite effects on them, i.e., the magnitude of CMR increases and the value of  $T_{MI}$  decreases with decreasing  $t$ .<sup>1-3</sup> It has been suggested<sup>4</sup> that the maximum CMR occurs in mixed-valent manganites with a tolerance factor  $t=0.96$ . However, most manganite that have  $t\approx 0.96$  possess relatively low values of  $T_{MI}$  ( $\sim 60$ – $150$  K). From the technological point of view, the challenge is to engineer materials which have the highest possible CMR at room temperature.

The application driven studies on manganite thin films were especially developed widely and profoundly over the past few years. Thin films of manganites exhibit properties quite different from the bulk due to the epitaxial strain induced by the lattice mismatch between the substrate and the bulk. One of the first remarkable findings in manganite thin films was the significant increase in CMR in  $\text{La}_{0.67}\text{Ca}_{0.33}\text{MnO}_3$  grown on  $\text{LaAlO}_3$  substrates.<sup>5</sup> The magnetoresistance ratio has been observed to strongly depend on the film thickness  $l$ ,<sup>5</sup> which is attributed to the variation in lattice parameter caused by epitaxial strain. Recent magnetotransport studies on manganite thin films grown on various substrates<sup>6</sup> have revealed that the magnetoresistance ratio shows weak thickness  $l$  dependence for  $l > 200 \text{ \AA}$  but it increases sharply with decreasing film thickness below  $200 \text{ \AA}$  for thin films, due to increased epitaxial strain. It is therefore desirable to grow manganite thin films with thicknesses be-

low some critical limit, in order to achieve the largest possible magnetoresistance. On the other hand, in bulk materials, maximum magnetoresistance occurs in manganites with tolerance factor  $t=0.96$ .<sup>3,4</sup> Considering the combined effect of film thickness and tolerance factor, one expects maximum magnetoresistance in the  $t=0.96$  ultrathin manganite films.

Now that the maximum magnetoresistance can be realized in the  $t=0.96$  ultrathin manganite films, the next step is to look for a suitable method to enhance  $T_{MI}$  in these materials. It has been generally accepted<sup>7-14</sup> that the  $T_{MI}$  (or the Curie temperature  $T_C$ ) can be effectively tuned by epitaxial strain. When the film is grown on a substrate whose lattice parameter is smaller (larger) than that of the bulk material, the epitaxial strain is expected to be compressive (tensile). Previous studies revealed<sup>9,10,13,14</sup> that compressive strain is an effective tool to enhance  $T_{MI}$  ( $T_C$ ) in manganite thin films. Since both epitaxially compressive strain and pressure increase  $T_{MI}$  ( $T_C$ ) in a similar way,<sup>14,15</sup> the significant enhancement of  $T_{MI}$  ( $T_C$ ) induced by compressive strain is expected in the materials which have a large pressure effect on  $T_{MI}$  ( $T_C$ ).

Figure 1 shows the magnetic ordering temperature and its pressure derivative taken from Refs. 16–19 vs doping  $x$ , as well as the tolerance factor  $t$ , obtained from the Shannon table<sup>20</sup> by taking the  $A$ -site cation ionic radii for 12-fold oxygen coordination, for the  $\text{La}_{1-x}\text{Sr}_x\text{MnO}_3$  system. The  $x=0.1$  compound with  $t=0.96$ , hence with the maximum magnetoresistance, has the highest value of the pressure derivative of  $T_C$ ,  $dT_C/dP$  (right vertical axis), which is one order of magnitude higher than the value of the optimally doped material ( $x=0.4$ ). Thus the ultrathin film of  $\text{La}_{0.9}\text{Sr}_{0.1}\text{MnO}_3$ , a material which has  $t=0.96$ , is a good candidate to have the largest compressive strain in enhancing  $T_C$  ( $T_{MI}$ ) as well as the maximum value of the magnetoresistance.  $\text{La}_{0.9}\text{Sr}_{0.1}\text{MnO}_3$  belongs to the distorted perovskitelike structure with orthorhombic  $Pbmm$  symmetry having lattice parameters<sup>21</sup>  $a/\sqrt{2}=3.922 \text{ \AA}$ ,  $b/\sqrt{2}=3.932 \text{ \AA}$ , and  $c/2=3.868 \text{ \AA}$ . In order to induce compressive strain in the film, we choose (100)-oriented  $\text{SrTiO}_3$  (STO) with lattice constant

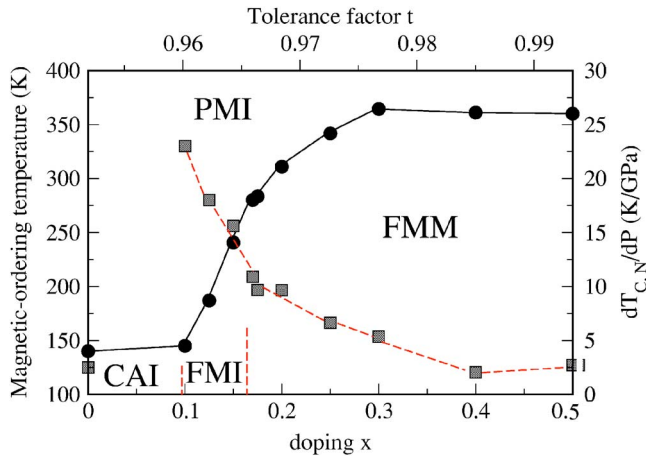


FIG. 1. (Color online) Phase diagram of the magnetic-ordering temperature (solid circles) and its pressure derivative (shaded squares) vs room-temperature tolerance factor  $t$  and the doping  $x$  in  $\text{La}_{1-x}\text{Sr}_x\text{MnO}_3$ . Phases include canted antiferromagnetic insulator (CAI), ferromagnetic insulator (FMI), ferromagnetic metal (FMM), and paramagnetic insulator (PMI). The lines are guides to the eye. The experimental data are taken from Refs. 16–19.

$a_0 = 3.905 \text{ \AA}$  as substrate materials since the in-plane lattice mismatch is 0.56%.

In this paper we show that compressive strain due to the lattice mismatch between the substrate and the bulk induces a spectacular increase in  $T_{MI}$  of ultrathin films of  $\text{La}_{0.9}\text{Sr}_{0.1}\text{MnO}_3$ , a material which has  $t = 0.96$ , hence, the maximum CMR amongst manganites, as well as the largest pressure derivative of  $T_{MI}$  ( $T_C$ ). The  $\text{La}_{0.9}\text{Sr}_{0.1}\text{MnO}_3$  ultrathin films grown epitaxially on (100)  $\text{SrTiO}_3$  substrates have  $T_{MI} = 308 \text{ K}$  while the material in bulk form has  $T_{MI} = 150 \text{ K}$ . We show that the strain-induced reduction of the Jahn-Teller distortion is responsible for this spectacular increase of  $T_{MI}$ .

## II. EXPERIMENT

Highly oriented thin films with thicknesses ranging from 50 to 2000  $\text{\AA}$  were deposited on (100)  $\text{SrTiO}_3$  substrates with pulsed laser deposition technique from a composite target  $\text{La}_{0.9}\text{Sr}_{0.1}\text{MnO}_3$ . The laser energy density on the target was  $2 \text{ J/cm}^2$  and the ablation rate was 5 Hz. The substrate was kept at a constant temperature of 850  $^\circ\text{C}$  during the deposition, which was carried out at a pressure of 0.40 mbar of oxygen. The films were *in situ* annealed at 940  $^\circ\text{C}$  in oxygen at 1.0 bar for 30 minutes. The surface morphology of these films was analyzed by atomic force microscopy (AFM) in air and room temperature. The film structures were examined by high resolution transmission electron microscopy (HRTEM) and x-ray diffraction (XRD). The dc resistivity of the films was measured in zero-field as well as in applied magnetic fields up to 14 T using the standard four-probe technique. The electrical current was applied in the film plane, perpendicular to the applied magnetic field. The magnetization was measured in a magnetic field parallel to the film plane using a superconducting quantum interference device (SQUID) magnetometer.

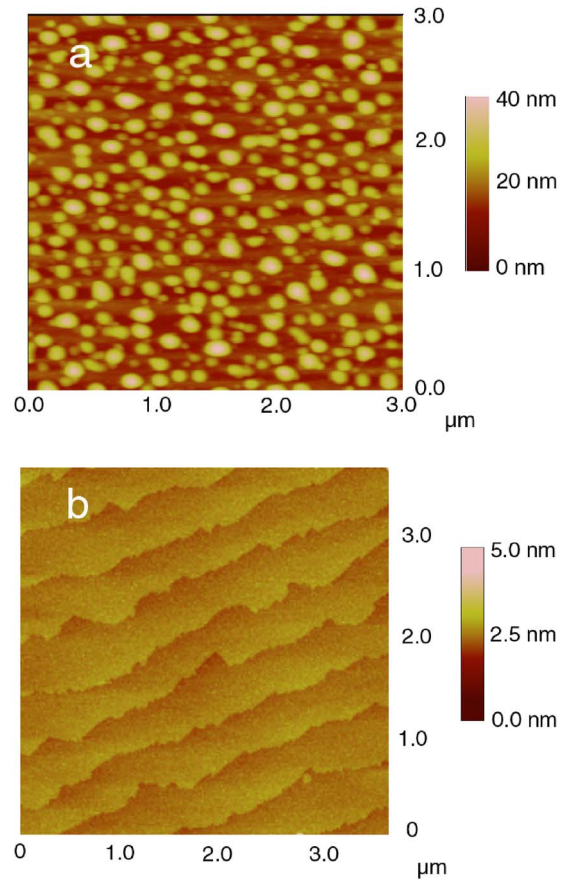


FIG. 2. (Color online) Typical AFM images of (a) 2000  $\text{\AA}$  and (b) 100  $\text{\AA}$   $\text{La}_{0.9}\text{Sr}_{0.1}\text{MnO}_3$  films epitaxially grown on (100)  $\text{SrTiO}_3$  substrates.

## III. RESULTS

Figure 2 shows AFM images of the surface morphology of 2000 and 100  $\text{\AA}$   $\text{La}_{0.9}\text{Sr}_{0.1}\text{MnO}_3$  films on (100)  $\text{SrTiO}_3$  substrates. The 2000  $\text{\AA}$  film shows a granularlike surface with rounded grains of typical in-plane size of 100 to 150 nm and height larger than 20 nm, as seen in Fig. 2(a). These islands are the result of a crossover from a 2D growth mode at small layer thickness into a 3D island growth at larger thickness, triggered by the relaxation of epitaxial strain. 2D growth for very thin layers is confirmed by AFM observations and by transmission electron microscopy (TEM). The AFM picture of Fig. 2(b) corresponds to a 10 nm thick sample and shows large flat terraces with a step height of 0.4 nm, characteristic of a 2D coverage of substrate miscut terraces.

TEM observations were carried out with a Philips CM200 microscope operated at 200 kV, and equipped with a field emission gun. Specimens in cross section geometry suitable for transmission electron microscopy (TEM) were obtained by conventional methods: mechanical grinding, dimpling, and Ar ion milling at a voltage of 5 kV and an incidence angle of 8 $^\circ$ . Figure 3(a) shows two images corresponding to the 50  $\text{\AA}$   $\text{La}_{0.9}\text{Sr}_{0.1}\text{MnO}_3$  thin film grown on a (100)  $\text{SrTiO}_3$  substrate. These images were obtained with the electron beam parallel to the interface and perpendicular to the (100)

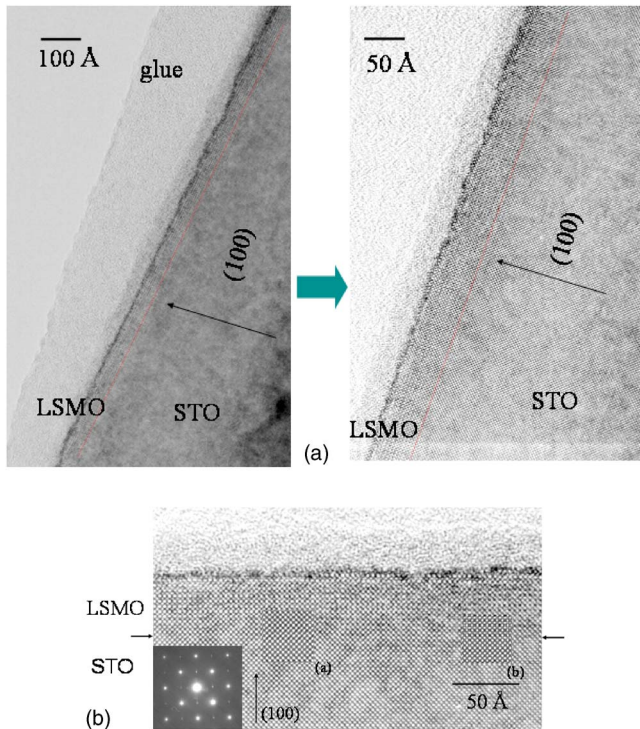


FIG. 3. (Color online) (A) TEM images for a 50 Å  $\text{La}_{0.9}\text{Sr}_{0.1}\text{MnO}_3$  thin film viewed along  $(100)_{\text{STO}}$ . Interfaces as marked with red dotted lines, are free of defects and have no dislocations. (B) HRTEM image of a 50 Å  $\text{La}_{0.9}\text{Sr}_{0.1}\text{MnO}_3$  thin film viewed along  $(100)_{\text{STO}}$ . The approximate position of the film-substrate interface is indicated by arrows. The inset shows the corresponding electron diffraction patterns. Insets (a) and (b) are the calculated images after simulating the interface structure.

direction of the substrate. The images denote high structural quality and sample homogeneity over long lateral distances. The film/substrate interface (marked with a red dotted line for clarity) is coherent and free of defects. This result is confirmed by high resolution observations [Fig. 3(b)]. The interface has been marked with black arrows. The left corner of Fig. 3(b) shows the corresponding electron diffraction pattern. Spots corresponding to substrate and film reflections cannot be distinguished from each other. This indicates that the lattice constants in the  $ab$  plane for the substrate and film are same within this resolution. Insets (a) and (b) to Fig. 3(b) show the calculated images after simulating the interface structure using defocus =  $-2000$  Å and specimen thicknesses along the electron beam direction of 500 and 600 Å, respectively. The simulated images were calculated using the MacTempas software. These observations confirmed the high quality and perfect epitaxy of the  $\text{La}_{0.9}\text{Sr}_{0.1}\text{MnO}_3$  thin films.

The temperature dependences of the resistivities of three films with different thicknesses are shown in Fig. 4. The resistivity of the 2000 Å film is insulatinglike but displays a clear hump at a temperature where the ferromagnetic transition happens, as confirmed by magnetization measurements. This resistivity plot is compatible with an heterogeneous film with metallic islands embedded in an insulating matrix. This may be indication of phase separation resulting from strain relaxation as previously observed by others.<sup>22,23</sup> The thinner

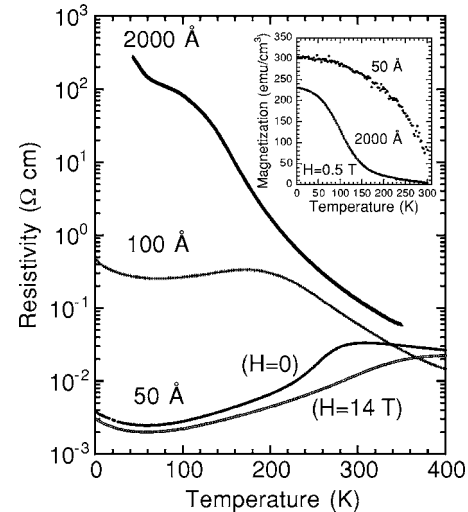


FIG. 4. Resistivity on a logarithmic scale versus temperature for  $\text{La}_{0.9}\text{Sr}_{0.1}\text{MnO}_3$  thin films with thicknesses of 2000, 100, and 50 Å in zero-field and a magnetic field of 14 T as indicated. The inset shows the magnetization (corrected for substrate contribution) in a magnetic field of 0.5 T of the 2000 and 50 Å  $\text{La}_{0.9}\text{Sr}_{0.1}\text{MnO}_3$  thin films. The curves have been measured by warming up in the magnetic field after zero field cooling.

films display the metal-insulator transition, characteristic of this class of materials. The resistivity is metallic below its corresponding  $T_{MI}$  and it is insulating above  $T_{MI}$ . At even lower temperatures, the resistivity first displays a minimum and then it has an upturn, which is probably associated to charge ordering.<sup>24</sup> These features are qualitatively similar to the behavior observed in bulk single crystals. We should emphasize that since the growth condition is the same for all the films studied, the difference of  $T_{MI}$  can only be explained by a change of film thickness rather than other factors.

Since the metal-insulator transition is usually accompanied by a transition from low-temperature ferromagnetic to high-temperature paramagnetic state,  $T_{MI}$  is approximately equal to the ferromagnetic transition temperature  $T_C$ . This is clearly shown by the main panel and its inset, which displays the magnetization curves of the films vs temperature, measured in 0.5 T. Increasing compressive strain, as a result of the reduction of film thickness, shifts  $T_{MI}$  and  $T_C$  to higher values and the charge ordering to lower temperatures. Moreover, the value of the low-temperature resistivity and the height of the resistivity peak are significantly suppressed with increasing compressive strain.

The ultrathin 50 Å  $\text{La}_{0.9}\text{Sr}_{0.1}\text{MnO}_3$  film has  $T_{MI}$  of 308 K measured in zero field, which is double the value of 150 K observed in bulk compounds.<sup>24</sup> An applied magnetic field of 14 T suppresses the resistivity and shifts  $T_{MI}$  towards higher temperatures, which gives rise to colossal magnetoresistance. As discussed above, the magnetoresistance has the maximum value in materials with this particular composition ( $x = 0.10$ ). Therefore, this 50 Å ultrathin film of  $\text{La}_{0.9}\text{Sr}_{0.1}\text{MnO}_3$  has a *room temperature* metal-insulator transition temperature and the maximum magnetoresistance. A doubling of  $T_{MI}$  in the present ultrathin film confirms the previous observation of the increase in  $T_{MI}$  ( $T_C$ ) with decreasing film thick-



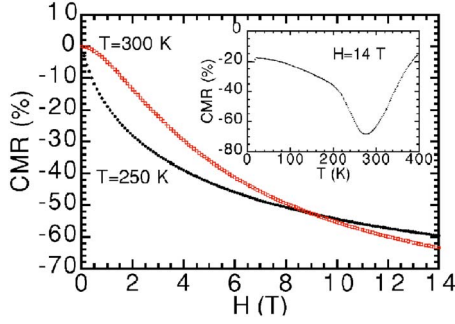


FIG. 5. (Color online) Magnetic field dependence of the magnitude of the colossal magnetoresistance  $CMR = [\rho(H) - \rho(0)]/\rho(0)$  for temperatures  $T=250$  and  $300$  K in a  $50$  Å  $La_{0.9}Sr_{0.1}MnO_3$  thin film. Inset: Temperature dependence of CMR in the same film for a magnetic field of  $14$  T.

ness in films with the same composition, where an increase of  $T_{MI}$  ( $T_C$ ) at around  $200$  K has been reported for a  $260$  Å film,<sup>13</sup> which was grown under conditions that were different than our growth conditions, and a  $200$  Å film, which was grown under conditions similar to our growth conditions.<sup>14</sup> To our knowledge, the present results provide the first convincing evidence for the remarkable strain effect on  $T_{MI}$  ( $T_C$ ) in manganite films.

Figure 5 is a plot of the magnetoresistance  $\Delta\rho(H)/\rho = [\rho(H) - \rho(0)]/\rho(0)$  at temperatures  $T=250$  and  $300$  K for the  $50$  Å ultrathin film, while its inset shows the temperature dependence of the  $\Delta\rho(H)/\rho$  in an applied field of  $14$  T. Noted that the absolute value of the  $\Delta\rho(H)/\rho$  increases with applied field even up to  $14$  T. The temperature dependence of the magnetoresistance shows that the absolute value of  $\Delta\rho(H)/\rho$  peaks near  $T_{MI}$ . For a given field strength, the  $\Delta\rho(H)/\rho$  at  $T=300$  K in the  $50$  Å ultrathin film is generally larger for other manganite films in literature. For example, the present ultrathin film exhibits  $\Delta\rho(H)/\rho$  of  $-22\%$ ,  $-33\%$ , and  $-36\%$  at  $T=300$  K in a field of  $3$ ,  $4.5$ , and  $5$  T, respectively. For comparison, there are reports of  $\Delta\rho(H)/\rho$  at  $T=300$  K of  $-11\%$  in a  $T_{MI}=355$  K  $La_{0.67}Sr_{0.33}MnO_3$  film at  $H=3$  T,<sup>26</sup>  $-13\%$  in a  $T_{MI}=230$  K  $La_{0.8}Sr_{0.2}MnO_3$  film at  $H=4.5$  T,<sup>27</sup> and  $-23\%$  in a  $T_{MI}=250$  K  $La_{0.7}Ca_{0.3}MnO_3$  film at  $H=5$  T.<sup>28</sup> We summarized these results in Table I.

#### IV. DISCUSSION

The occurrence of the metal-insulator transition in manganites has been explained in terms of two competing ef-

fects: the double-exchange interaction,<sup>25</sup> which increases the electrons' kinetic energy and, hence, their delocalization, and the Jahn-Teller coupling, which tends to localize the carriers in a local lattice distortion.<sup>29</sup> Diffraction measurements<sup>30</sup> as a function of  $T$ ,  $P$ , and  $r_A$  have shown that the *reduction* of the Jahn-Teller distortion of the  $MnO_6$  octahedra favors the enhancement of the metallic character, hence, the *increase* of  $T_C$ . The reduction of the Jahn-Teller distortion can be realized if the octahedra are forced to be undistorted and the Mn-O-Mn angle approaches  $180^\circ$ . Epitaxial strain of thin films due to lattice mismatch between the film and the substrate is an effective method in adjusting the Jahn-Teller distortion through the change of the Mn-O bond length and the Mn-O-Mn angle. If there is a compressive strain in plane there is an expansion out of plane because of the Poisson effect. The net effect on the MnO bonds is to flatten the Mn-O-Mn bond angle (approach  $180^\circ$ ).

We now show that the enhancement of  $T_C$  ( $T_{MI}$ ) observed in the present material can be understood on the basis of the combined effect of double-exchange and Jahn-Teller coupling. The double-exchange model predicts that there is a close relationship between  $T_C$  and the one-electron bandwidth ( $W$ ) of the  $e_g$  band in the strong-coupling limit; i.e.,  $T_C \propto W$ .<sup>19</sup> The large pressure coefficient of the lightly doped  $La_{1-x}Sr_xMnO_3$  indicates that this system is, indeed, in the strong-coupling region. Jahn-Teller polarons are formed when the Jahn-Teller stabilization energy becomes comparable to the bare conduction bandwidth. The polaronic nature of the conduction affects bandwidth as described by  $W_{eff} \propto W \exp(-\gamma E_P/\hbar\omega)$ ,<sup>31</sup> where  $\gamma$  is a positive constant,  $E_P$  is the formation energy of Jahn-Teller polarons, and  $\omega$  is the characteristic frequency of the optical phonon mode. Given the large value of  $E_P$  for the  $Mn^{3+}$  of  $0.5$  eV, polaronic effects in conduction are expected in manganites as in fact have been observed by Zhao *et al.*<sup>32</sup> The giant isotope effect on  $T_C$  of manganites reflects the importance of electron phonon interactions and shows that for Jahn-Teller polaronic conduction  $T_C \propto W_{eff}$  (rather than  $T_C \propto W$  for bare conduction). The strain coefficient of  $T_C$  is then given by

$$\frac{d \ln T_C}{d \epsilon} = \frac{d \ln W}{d \epsilon} - 2\alpha \left( \frac{d \ln E_P}{d \epsilon} - \frac{d \ln \omega}{d \epsilon} \right), \quad (1)$$

where the isotope exponent  $\alpha \equiv 0.5 \gamma E_P/\hbar\omega$  and the in-plane lattice strain  $\epsilon = (d_{bulk} - d_{film})/d_{bulk}$ , with  $d = (a+b)/2\sqrt{2}$  the in-plane lattice parameter.

TABLE I. Summary of the magnetoresistivity  $\Delta\rho(H)/\rho = [\rho(H) - \rho(0)]/\rho(0)$  measured at  $T=300$  K and the metal-insulator transition temperature ( $T_{MI}$ ) of our  $50$  Å  $La_{0.9}Sr_{0.1}MnO_3$  film and other manganite films reported in Refs. 26–28.

Film	Substrate	$T_{MI}$ (K)	$\Delta\rho(3 \text{ T})/\rho$	$\Delta\rho(4.5 \text{ T})/\rho$	$\Delta\rho(5 \text{ T})/\rho$
$La_{0.9}Sr_{0.1}MnO_3$	(100) SrTiO <sub>3</sub>	308	$-22\%$	$-33\%$	$-36\%$
$La_{0.8}Sr_{0.2}MnO_3$	(100) LaAlO <sub>3</sub>	230		$-13\%$	
$La_{0.67}Sr_{0.33}MnO_3$	(111) Si	355	$-11\%$		
$La_{0.7}Ca_{0.3}MnO_3$	(100) LaAlO <sub>3</sub>	250			$-23\%$

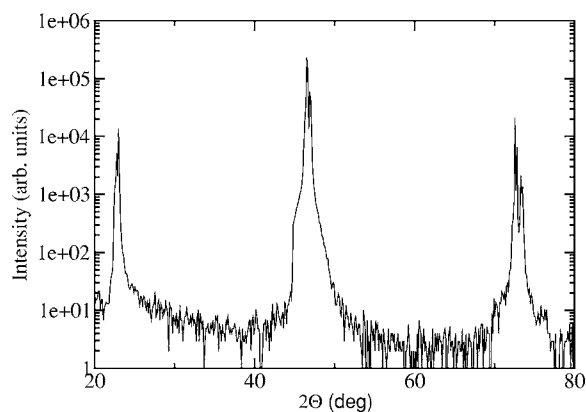


FIG. 6. X-ray-diffraction pattern ( $\Theta$ - $2\Theta$  scan) of a 2000 Å  $\text{La}_{0.9}\text{Sr}_{0.1}\text{MnO}_3$  film grown on a (100)  $\text{SrTiO}_3$  substrate.

An analysis of the film thickness dependence of lattice parameters<sup>33</sup> has shown that the lattice parameters for the thinnest films exhibit the largest deviations from those of the bulk, with the in-plane values at or near those of the substrates. As film thickness increases, and lattice relaxation takes place, both in-plane and out-of-plane lattice parameters tend to deviate away from those of the substrates towards the bulk values. Such behavior is further confirmed by the XRD measurements on our 2000 Å  $\text{La}_{0.9}\text{Sr}_{0.1}\text{MnO}_3$  film (shown in Fig. 6). The XRD pattern of this thick film gives a  $c$ -axis lattice parameter of 3.869 Å which is very close to that of 3.868 Å in the bulk material.<sup>21</sup> It is therefore reasonable to take  $d_{\text{film}} = d_{\text{STO}} = 3.905$  Å and  $T_C = 308$  K for the 50 Å ultra-thin film, and  $d_{\text{film}} = d_{\text{bulk}} = 3.927$  Å (Ref. 21) and  $T_C = 150$  K for the 2000 Å thick film, in which the strain is relaxed. Then we estimate  $d \ln T_C / d\epsilon = 188$ . Based on this value and the measured  $d \ln T_C / dP$  of  $0.16 \text{ GPa}^{-1}$  for this material,<sup>17</sup> we obtain the compressibility  $\kappa_d = 8.5 \times 10^{-4} \text{ GPa}^{-1}$ .

Raman spectra studies show that the high frequency  $B_{2g}$  mode at  $609 \text{ cm}^{-1}$  corresponds to an in-plane O(2) stretching mode (a Jahn-Teller phonon).<sup>34</sup> This stretching mode is the most sensitive to pressure with an initial pressure coefficient,  $d \ln \omega / dP = 0.01 \text{ GPa}^{-1}$ ,<sup>34</sup> thus yielding  $d \ln \omega / d\epsilon = 11.8$ . In perovskites,<sup>30</sup>  $W \propto \cos \phi / d_{\text{Mn-O}}^{3.5}$  with  $\phi = (\pi - \langle \text{Mn-O-Mn} \rangle) / 2$  being the tilt angle in the plane of the bond and  $d_{\text{Mn-O}}$  the Mn-O bond length. According to neutron diffraction,<sup>30</sup> the compressibility of  $\cos \phi$  is one order of magnitude smaller than that of  $d_{\text{Mn-O}}$  and can be neglected. In this case,  $d \ln W / d\epsilon = 3.5$ . The oxygen isotope exponent  $\alpha$  is 0.2 in  $\text{La}_{0.9}\text{Sr}_{0.1}\text{MnO}_3$ .<sup>32</sup> With these values of the three strain coefficients and of  $\alpha$ , Eq. (1) gives  $d \ln E_P / d\epsilon = -449$ . Two main results follow. First, the polaron formation energy ( $E_P$ ) decreases significantly with increasing compressive strain. This implies that the Jahn-Teller distortion decreases significantly with increasing compressive strain. Second, the strain coefficient of  $E_P$  ( $d \ln E_P / d\epsilon$ ) is the dominant contribution to the strain coefficient of the ferromagnetic transition temperature ( $d \ln T_C / d\epsilon$ ). Therefore, the strain driven enhancement of  $T_C$  ( $T_{MI}$ ) in the present thin films mainly results from the strain induced reduction of the Jahn-Teller distortion.

Previous transport studies<sup>14</sup> have shown that  $E_P$  decreases and  $T_C$  increases with increasing compressive strain for the

$\text{La}_{0.9}\text{Sr}_{0.1}\text{MnO}_3$  thin films with thicknesses between 200 and 750 Å. A similar behavior was observed with applied hydrostatic pressure.<sup>15</sup> There is almost a linear relationship between  $E_P$  and  $T_C$  in both cases. With the values of the strain coefficients of  $T_C$  and  $E_P$  determined above, we estimate  $d \ln E_P / d \ln T_C = -2.4$  in the present material. This value agrees well with the value of  $-3.2$  from the pressure studies of  $\text{La}_{0.65}\text{Ca}_{0.35}\text{MnO}_3$ .<sup>15</sup>

The strain effect in manganite films is usually interpreted within the framework of the double-exchange theory alone. Since the compressed (expanded) Mn-O bond lengths under the compressive (tensile) strain lead to the increase (decrease) of electron transfer or bandwidth,  $T_C$  is then increased (decreased), accordingly. This explanation may be plausible for the epitaxial films of  $\text{La}_{1-x}\text{Sr}_x\text{MnO}_3$  and  $\text{La}_{1-x}\text{Ca}_x\text{MnO}_3$  ( $x \sim 1/3$ ). This is because there is only a small strain effect in nearly optimal-doped films, due to the relatively small pressure derivatives of  $T_C$  for these films, in comparison to the large strain effects we find in the slightly doped materials shown in Fig. 1. Therefore, it is also not surprising to observe an almost constant  $T_C$  in the  $\text{La}_{1-x}\text{Ba}_x\text{MnO}_3$  ( $x = 0.3, 0.33$ ) films over a wide compressive strain range through the change of film thickness.<sup>35</sup> From the above detailed analysis, we learn that the strain-induced change of  $W$  can not account for the significant change of  $T_C$  ( $T_{MI}$ ). However, the strain-induced reduction of the Jahn-Teller distortion mainly contributes to such a significant increase of  $T_C$  ( $T_{MI}$ ) in our films.

Recently, Ahn *et al.*<sup>36</sup> proposed a natural mechanism for the strain-induced metal-insulator phase coexistence in manganites, in which the phase with short- and long-wavelength lattice distortion is insulating, and that without lattice distortion is metallic. If the multiphase coexistence is indeed a self-organized intrinsic feature of manganites, compressive strain would modify the energy landscape in favor of the undistorted ferromagnetic metallic state and increase the volume fraction of the metallic regions. As a result, an increase of  $T_C$  ( $T_{MI}$ ) is expected in films in which the compressive strain is induced by the lattice mismatch. The experimental fact that a significant increase of  $T_C$  ( $T_{MI}$ ) mainly originates from the reduction of the Jahn-Teller distortion under compressive strain is consistent with this newly proposed theoretical model.

We would like to comment on another possibility that could contribute to the observed significant increase of  $T_C$  ( $T_{MI}$ ) in our films triggered by compressive strain, namely, the orbital degree of freedom. The role of the orbital degree of freedom was emphasized by Kanki *et al.*<sup>37</sup> in the study of an anomalous strain effect in  $\text{La}_{0.8}\text{Ba}_{0.2}\text{MnO}_3$  films. By modifying the transfer integral to include the orbital contribution from  $d_{x^2-y^2}$  and  $d_{3z^2-r^2}$ , they were able to interpret the observed tensile-strain induced increase of  $T_C$  in their films. According to their calculation, a 0.31–0.52 % change of the in-plane lattice constant would lead to a 0.02–0.03 % change of  $T_C$ . In our case, there is a 0.56% change of the in-plane lattice constant. The orbital degree of freedom is not sufficient, by far, to account for the 105% increase of  $T_C$ .

It should be pointed out that the in-plane compressive strain  $\epsilon$  has been used to estimate  $d \ln T_C / d\epsilon$  and  $d \ln E_P / d\epsilon$

in our analysis. This treatment is reasonable since the other relevant physical quantities such as phonon frequency  $\omega$  and structural parameters are obtained from hydrostatic pressure measurements where both the in-plane and out-of-plane lattice parameters would be compressed under pressure. When a system is under compressive strain, one expects a decrease of the in-plane lattice parameters, but an expansion of the lattice along the  $c$ -axis direction normal to the substrate. The relationship between the in-plane strain  $\epsilon$  and bulk strain  $\epsilon_B$  ( $\equiv \epsilon_{xx} + \epsilon_{yy} + \epsilon_{zz}$ ) is given by  $\epsilon_B = 2(1 - \nu)\epsilon$  with  $\nu$  the Poisson's ratio. The value of  $\nu$  is usually estimated from the elastic moduli, i.e.,  $\nu = C_{12}/(C_{11} + C_{12})$ . Ultrasonic measurements<sup>38</sup> of a single crystal of  $\text{La}_{0.88}\text{Sr}_{0.12}\text{MnO}_3$ , with the composition near our lightly doped material, give  $C_{11} = 17.3 \times 10^{11}$  erg/cm<sup>3</sup> and  $(C_{11} - C_{12})/2 = 3.5 \times 10^{11}$  erg/cm<sup>3</sup> at  $T = 300$  K. The obtained Poisson's ratio  $\nu$  of 0.37 is very close to the reported 0.36 in ultrathin  $\text{Pr}_{0.7}\text{Sr}_{0.3}\text{MnO}_3$  films.<sup>39</sup> If we use  $\nu = 0.37$  for our  $\text{La}_{0.9}\text{Sr}_{0.1}\text{MnO}_3$  films, we get  $d \ln T_C/d\epsilon_B = 149$ . This experimental value is ten times larger in magnitude than the theoretical predication<sup>7</sup> in the CMR regime of the dimensionless electron-phonon coupling constant  $\lambda \approx 1$ , indicating that the theoretical calculations themselves need improvement.

Notice that the value of  $d \ln T_C/d\epsilon_B$  estimated from the bulk strain is smaller than  $d \ln T_C/d\epsilon$  from the in-plane strain. Assuming that the hydrostatic pressure data are still applicable, we have  $d \ln W/d\epsilon_B = 3.5$  and  $d \ln \omega/d\epsilon_B = 9.3$ . By substituting these values into Eq. (1), we obtain a  $d \ln E_P/d\epsilon_B$  of  $-354$ . Again, we have  $d \ln E_P/d \ln T_C = -2.4$ . Good agreement with the hydrostatic pressure measurements<sup>15</sup> provides convincing evidence for the reduction of

the Jahn-Teller distortion under compressive strain in favor of the increase of  $T_C$ . Since  $d \ln E_P/d\epsilon_B$  dominates the contribution to  $d \ln T_C/d\epsilon_B$ , the bulk strain state does not affect the conclusion drawn from the in-plane strain data. It is clear that the theoretical framework presented here captures the basic physics of the strain effect in manganese films.

## V. CONCLUSION

The present study opens a new avenue for engineering materials with maximum magnetoresistance above room temperature. We emphasize that the strain driven enhancement of  $T_{MI}$  in the  $\text{La}_{0.9}\text{Sr}_{0.1}\text{MnO}_3$  thin films is a natural result and a successful application of the strain effect in manganites. Our results strongly indicate that the strong electron-phonon coupling stemming from a Jahn-Teller splitting of the  $\text{Mn}^{3+}$  ion plays a crucial role in addition to double-exchange in the CMR of these manganites. Other possibilities that contribute to the enhancement of  $T_C$  such as hopping integral alone, orbital degree of freedom, and multiphase coexistence are also discussed. We demonstrate that the in-plane strain state is suitable for describing the underlying physics of the strain effect in manganese films.

## ACKNOWLEDGMENTS

The work was supported at KSU by the U.S. National Science Foundation Grant No. DMR-0406471. X.J.C. also acknowledges support from the U.S. Department of Energy under Grant No. DEFG02-02ER4595.

- 
- <sup>1</sup>W. Archibald, J.-S. Zhou, and J. B. Goodenough, *Phys. Rev. B* **53**, 14445 (1996).
- <sup>2</sup>H. Y. Hwang, T. T. M. Palstra, S.-W. Cheong, and B. Batlogg, *Phys. Rev. B* **52**, 15046 (1995).
- <sup>3</sup>R. Mahesh, R. Mahendiran, A. K. Raychaudhuri, and C. N. R. Rao, *J. Solid State Chem.* **120**, 204 (1995).
- <sup>4</sup>J.-S. Zhou, W. Archibald, and J. B. Goodenough, *Nature (London)* **381**, 770 (1996).
- <sup>5</sup>S. Jin, T. H. Tiefel, M. McCormack, H. M. O'Bryan, L. H. Chen, R. Ramesh, and D. Schurig, *Appl. Phys. Lett.* **67**, 557 (1995).
- <sup>6</sup>H. S. Wang, E. Wertz, Y. F. Hu, Q. Li, and D. G. Schlom, *J. Appl. Phys.* **87**, 7409 (2000).
- <sup>7</sup>A. J. Millis, T. Darling, and A. Migliori, *J. Appl. Phys.* **83**, 1588 (1998).
- <sup>8</sup>H. L. Ju, C. Kwon, Q. Li, R. L. Greene, and T. Venkatesan, *Appl. Phys. Lett.* **65**, 2108 (1994).
- <sup>9</sup>T. Y. Koo, S. H. Park, K.-B. Lee, and Y. H. Jeong, *Appl. Phys. Lett.* **71**, 977 (1997).
- <sup>10</sup>C. Kwon, M. C. Robson, K.-C. Kim, J. Y. Gu, S. E. Lofland, S. M. Bhagat, Z. Trajanovic, M. Rajeswari, T. Venkatesan, A. R. Kratz, R. D. Gomez, and R. Ramesh, *J. Magn. Magn. Mater.* **172**, 229 (1997).
- <sup>11</sup>R. A. Rao, D. Lavric, T. K. Nath, C. B. Eom, L. Wu, and F. Tsui, *J. Appl. Phys.* **85**, 4794 (1999).
- <sup>12</sup>W. Prellier, A. M. Haghiri-Gosnet, B. Mercey, Ph. Lecoeur, M. Hervieu, Ch. Simon, and B. Raveau, *Appl. Phys. Lett.* **77**, 1023 (2000).
- <sup>13</sup>F. S. Razavi, G. Gross, H.-U. Habermeier, O. Lebedev, S. Amelinckx, G. Van Tendeloo, and A. Vigliante, *Appl. Phys. Lett.* **76**, 155 (2000).
- <sup>14</sup>X. J. Chen, S. Soltan, H. Zhang, and H.-U. Habermeier, *Phys. Rev. B* **65**, 174402 (2002).
- <sup>15</sup>B. Lorenz, A. K. Heilman, Y. S. Wang, Y. Y. Xue, C. W. Chu, G. Zhang, and J. P. Franck, *Phys. Rev. B* **63**, 144405 (2001).
- <sup>16</sup>L. Pinsard-Gaudart, J. Rodríguez-Carvajal, A. Daoud-Aladine, I. Goncharenko, M. Medarde, R. I. Smith, and A. Revcolevschi, *Phys. Rev. B* **64**, 064426 (2001).
- <sup>17</sup>R. Senis, V. Laukhin, B. Martínez, J. Fontcuberta, X. Obradors, A. A. Arsenov, and Y. M. Mukovskii, *Phys. Rev. B* **57**, 14680 (1998).
- <sup>18</sup>A. E. Petrova, E. S. Itskevich, V. A. Ventcel', V. F. Kraidenov, and A. V. Rudnev, *Low Temp. Phys.* **27**, 831 (2001) [*Fiz. Nizk. Temp.* **27**, 1123 (2001)].
- <sup>19</sup>Y. Moritomo, A. Asamitsu, and Y. Tokura, *Phys. Rev. B* **51**, R16491 (1995).
- <sup>20</sup>R. D. Shannon, *Acta Crystallogr., Sect. A: Cryst. Phys., Diff., Theor. Gen. Crystallogr.* **32**, 751 (1976).
- <sup>21</sup>D. E. Cox, T. Iglesias, E. Moshopoulou, K. Hirota, K. Takahashi, and Y. Endoh, *Phys. Rev. B* **64**, 024431 (2001).
- <sup>22</sup>A. Biswas, M. Rajeswari, R. C. Srivastava, T. Venkatesan, R. L.

- Greene, Q. Lu, A. L. de Lozanne, and A. J. Millis, *Phys. Rev. B* **63**, 184424 (2001).
- <sup>23</sup>A. Biswas, M. Rajeswari, R. C. Srivastava, Y. H. Li, T. Venkatesan, R. L. Greene, and A. J. Millis, *Phys. Rev. B* **61**, 9665 (2000).
- <sup>24</sup>A. Urushibara, Y. Moritomo, T. Arima, A. Asamitsu, G. Kido, and Y. Tokura, *Phys. Rev. B* **51**, 14103 (1995).
- <sup>25</sup>C. Zener, *Phys. Rev.* **82**, 403 (1951).
- <sup>26</sup>O. J. González, G. Bistué, E. Castaño, and F. J. Gracia, *J. Magn. Magn. Mater.* **222**, 199 (2000).
- <sup>27</sup>N. Sharma, A. K. Nigam, R. Pinto, N. Venkataramani, S. Prasad, G. Chandra, and S. P. Pai, *J. Magn. Magn. Mater.* **154**, 296 (1996).
- <sup>28</sup>M. F. Hundley, M. Hawley, R. H. Heffner, Q. X. Jia, J. J. Neumeier, J. Tesmer, J. D. Thompson, and X. D. Wu, *Appl. Phys. Lett.* **67**, 860 (1995).
- <sup>29</sup>A. J. Millis, P. B. Littlewood, and B. I. Shraiman, *Phys. Rev. Lett.* **74**, 5144 (1995).
- <sup>30</sup>P. G. Radaelli, G. Iannone, M. Marezio, H. Y. Hwang, S.-W. Cheong, J. D. Jorgensen, and D. N. Argyriou, *Phys. Rev. B* **56**, 8265 (1997).
- <sup>31</sup>A. S. Alexandrov and N. F. Mott, *Int. J. Mod. Phys. B* **8**, 2075 (1994).
- <sup>32</sup>G.-M. Zhao, K. Conder, H. Keller, and K. A. Müller, *Nature (London)* **381**, 676 (1996).
- <sup>33</sup>R. A. Rao, D. Lavric, T. K. Nath, C. B. Eom, L. Wu, and F. Tsui, *Appl. Phys. Lett.* **73**, 3294 (1998).
- <sup>34</sup>A. Congeduti, P. Postorino, E. Caramagno, M. Nardone, A. Kumar, and D. D. Sarma, *Phys. Rev. Lett.* **86**, 1251 (2001).
- <sup>35</sup>J. Zhang, H. Tanaka, T. Kanki, J.-H. Choi, and T. Kawai, *Phys. Rev. B* **64**, 184404 (2001).
- <sup>36</sup>K. H. Ahn, T. Lookman, and A. R. Bishop, *Nature (London)* **428**, 401 (2004).
- <sup>37</sup>T. Kanki, H. Tanaka, and T. Kawai, *Phys. Rev. B* **64**, 224418 (2001).
- <sup>38</sup>H. Hazama, T. Goto, Y. Nemoto, Y. Tomioka, A. Asamitsu, and Y. Tokura, *Phys. Rev. B* **62**, 15012 (2000).
- <sup>39</sup>I. MacLaren, Z. L. Wang, H. S. Wang, and Q. Li, *Appl. Phys. Lett.* **80**, 1406 (2002).